RSC Advances

The hydrophobic interaction between laurel alkanolamide micelles and hydrophobically associating polyacrylamide enhances the formation of network structure and the viscosity of the mixed solution increases in large electrolyte concentration range.

Synergistic mechanism between laurel alkanolamide and hydrophobically associating polyacrylamide in solutions with high salinity

Quanhua Deng[a], Haiping Li[b], Xulong Cao[c], Yong Yang[c], Xinwang Song[c], Ying Li[a*]

[a]*Key Laboratory for Colloid and Interface Chemistry of Education Ministry, Shandong University, Jinan 250100, P.R. China;*

[b]*National Engineering Technology Research Center for Colloidal Materials, Shandong University, Jinan 250100, P.R. China;*

[c]*Geological Scientific Research Institute, Shengli Oilfield, Dongying 257015, P.R. China.*

[*] To whom correspondence should be addressed

Email: yingli@sdu.edu.cn

Telephone: +86-531-88362078

Fax: +86-531-88362078

Running title: Synergism between LAA and HA-PAM

24

25   **Abstract**

26   Synergism of water-soluble hydrophobically associating polyacrylamide

27   (HA-PAM) with nonionic surfactant laurel alkanolamide (LAA) was investigated via

28   the rheology, fluorescence spectroscopy and dissipative particle dynamics (DPD)

29   simulation methods. The viscosity and elasticity of HA-PAM solutions increased in

30   large LAA concentration range, which was principally ascribed to the crosslinking

31   effect of LAA by aggregating to the hydrophobic chains of HA-PAM molecules as

32   confirmed by the DPD simulation and experimental results. The crosslinking effect

33   was enhanced in the presence of appropriate amount of electrolyte or with increasing

34   temperature in the studied temperature range of 20–70 °C. Thus, the LAA not only

35   significantly enhanced the salt resistance of HA-PAM but also retarded the decrease

36   of the viscosity and elasticity of the HA-PAM solutions at high temperature. The

37   HA-PAM/LAA binary systems exhibit great potential for application in tertiary oil

38   recovery of oil fields with high salinity.

39   **Keyword:** hydrophobically associating polyacrylamide, laurel alkanolamide, salt

40   resistance, synergism

41

42

1. Introduction

43

44   Polymer and polymer/surfactant flooding systems have been extensively used in

45   enhanced oil recovery (EOR),[1] in which polymers are being used as thickeners to

46   increase the viscosity of the flooding system and adjust the mobility ratio of water and

47   oil phase. Polymers are indispensable for the high oil displacement efficiency of the

48   flooding systems. Partially hydrolyzed polyacrylamide (HPAM)[2] is the most widely

49   used polymer in EOR, but the poor salt and shear resistance of HPAM limit its

50   application in reservoirs with high salinity.

51   In recent years, polymers containing salt resistance components such as

52   amphoteric or nonionic side groups[3, 4] have been reported with strong salt and shear

53   resistance. More exciting progress comes from the advance of the comb-shaped,[5]

54   hydrophobically associating[6] polymers, which could form reversible networks,

55   resulting in a dramatic increase in apparent viscosity even at a low concentration or

56   under high salinity, and attracted the most interest of researchers. According to the

57   literature reports,[7] hydrophobically associating polyacrylamide (HA-PAM) exhibited

58   much better salt resistance than HPAM and have showed great potential for

59   application in reservoirs with high salinity.

60   In most of the actual practices, EOR for example, polymers were used, combined

61   with surfactant. The interaction between surfactants and polymers was an interesting

62   topic, attracting much more attention for a long time. Surfactants have strong

3

63   influences on the rheological properties[8] and salt resistance of polymeric solutions.[9-11]

64   The polymer/surfactant systems with opposite charge[12-15] have been paid much

65   attention. The viscosity of the solution could be greatly improved because of the inter-

66   or intra- molecular cross-links driven by the electrostatic attracting interactions. But

67   the synergistic effect is very sensitive to the concentration ratio of the surfactants and

68   polymers, and these mixed solutions always exhibit a bad salt resistance, because the

69   electrostatic interactions are sensitive to electrolytes, and minor electrolytes lead to a

70   sharp decrease of the viscosity of the solutions.[16] The combination of the

71   polyelectrolytes and ionic surfactants with the same charge or nonionic surfactants

72   were also reported. Hydrophobic interaction was the driving force to enhance the

73   formation of molecular network, and some complex exhibited better salt resistance.[11,

74   17] The synergetic effect between HA-PAM and surfactants is still unclear, and the

75   related reports were rare. To seek appropriate surfactants to cooperate with HA-PAM

76   for further enhancing its salt resistance and oil displacement capability is desired in

77   practical areas.

78   In this study, the rheological properties of mixed solutions of HA-PAM and

79   anionic, amphoteric and nonionic surfactants were investigated. The salt resistance of

80   HA-PAM solutions was greatly enhanced in the presence of nonionic surfactant laurel

81   alkanolamide (LAA). The synergism between HA-PAM and LAA were investigated

82   by combining experimental and molecular simulation methods. The HA-PAM/LAA

83   (H/L) binary system exhibits high thickening capacity in large concentration ratio or

84 under high salinity. This system has great potential for application as a

85 polymer/surfactant flooding system in high salinity reservoirs.

86 **2. Materials and methods**

87 **2.1. Materials**

88   HA-PAM with a viscosity-averaged molecular weight of 3.6×10^5 and

89 cocamidopropyl betaine (CAB, 30% aqueous solution, 99% purity) were provided

90 by Geological Scientific Research Institute of Shengli oil field (Sinopec, China).[7]

91 Laurel alkanolamide (LAA) was synthesized in our lab and purified according to Ref.

92 18.[18] Sodium dodecyl sulfate (SDS, 99% purity) was obtained from Cxbio

93 Biotechnology Co. Ltd. (China). Dodecyl sulphobetaine (DSB, analytical pure) was

94 synthesized and purified by Dr. J. Chen in Jin Ling Petrochemical Co. (Sinopec,

95 China). Nonaethylene glycol monododecyl ether ($C_{12}E_9$, 99% purity) was purchased

96 from Sigma-Adrich. Deionized water was used in all the experiments. Chemical

97 structures of HA-PAM and LAA are shown in Fig. 1. Structures of the other

98 surfactants are shown in Fig. S1.

99

5
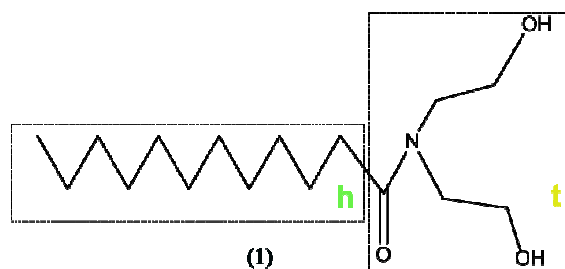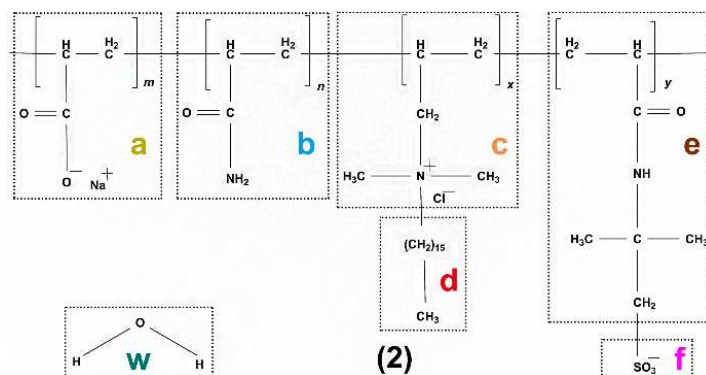
Fig. 1 Structures of LAA (1) and HA-PAM (2) with mole percent of *m, n, x* and *y* to

be 10, 80, 0.5 and 9.5 mol%, respectively. In DPD simulation, segments of HA-PAM

and LAA molecules are represented by beads, labeled as 'a', 'b', 'c', 'd', 'e', 'f', 'h'

and 't', respectively. The water molecule is labeled as 'w'.

        The HA-PAM and LAA stock solutions with concentrations of 0.2% and 1%

were prepared by dissolving 0.2 g HA-PAM and 1.0 g LAA in 99.8 and 99.0 g

deionized water, respectively. Solutions with low concentrations of HA-PAM and/or

LAA were obtained via the dilution of the stock solutions. The pH values of all the

solutions are 7.28 ± 0.19. The NaCl concentrations of solutions were adjusted by

adding 10 or 1% NaCl bulk solutions. The HA-PAM concentration is 0.1% in all the

related solutions in this paper unless special explanation. HA-PAM solutions

containing pyrene (about 3.03×10^{-4} g·L^{-1}) were prepared by adding 20 μL of 0.15

g·L^{-1} pyrene ethanol solution to 10 ml of 0.1% HA-PAM aqueous solution.

2.2. Rheological measurement

        Rheological measurements were carried out on a Haake RS75 Rheometer

117   (Germany) with a Z41 Ti coaxial cylinder sensor system. All of the samples were

118   rested for more than 12 h to eliminate the bubbles before measurement.

119   In the steady-state shearing experiment, the viscosity was measured at the shear

120   rates ($\dot{\gamma}$) ranging from 0 to 1000 s^{-1} with a check gradient of 0.5 ($\Delta\tau/\tau)/\Delta t$% where τ

121   and t is the shear stress and time, respectively, and the maximum waiting time for

122   each shear rate step was 20 s. The frequency sweep measurements were carried out at

123   the angular frequency (ω) of 0.05–100 rad·s^{-1} and stress of 0.04 Pa (in the linear

124   viscoelastic region). The equilibrium values of dynamic viscosity ($|\eta^*|$) and moduli

125   (G' and G'') were measured at $\omega = 0.2$ rad·s^{-1} in the linear viscoelastic region. The

126   experiment temperature was controlled to be 25.0 ± 0.1 °C, unless the temperature

127   effect was investigated.

128   The "gain in viscosity",[19] S_η is defined to denote the interacting strength between

129   HA-PAM and LAA:

130       $$S_\eta = \frac{\eta_{H/L}}{\eta_H}$$ (1)

131   where $\eta_{H/L}$ and η_H are the viscosity of H/L and HA-PAM solutions,[7] respectively.

132   Herein, $S_\eta > 1$ means the interaction increases the solution viscosity; on the contrary,

133   the interaction causes the decrease of solution viscosity.

134   **2.3. Fluorescence and surface tension measurements**

135   Fluorescence spectra of solutions were detected with a Perkin-Elmer LS-55

136   spectrofluorometer using a quartz cuvette (1.0 cm × 1.0 cm). The excitation and

137   emission slit widths were set at 7.5 nm. The emission spectra were recorded from 350

138   to 650 nm with excitation wavelength fixed at 335 nm. The fluorescence intensity

139   ratio at 373 and 384 nm, namely, I_1/I_3 served as a parameter representing the

140   micropolarity of aggregates. Pyrene was used as a fluorescent probe with the

141   concentration of 3.03×10^{-4} g·L^{-1}.

142   Surface tension measurements of various concentrations of LAA solutions were

143   performed on a K100 Processor Tensiometer (Krüss Co., Germany) using the

144   Wilhelmy ring at 30.0 ± 0.1 °C. Before each measurement, the plate was carefully

145   cleaned with deionized water and flamed. The surface tension of deionized water was

146   measured to calibrate the tensiometer and to check the cleanliness of the sample pool.

147   **2.4. DPD simulation**

148   Simulations were carried out with the DPD package from Accelrys (version 5.0),

149   [20]. A cubic cell of size $20 \times 20 \times 20$ R_c^3 was built, where $R_c = 9.5$ was the cut-off

150   radius. 20000 time steps per simulation were set to assure the system attained

151   dynamic equilibrium. The number density and the spring constant between different

152   beads were 3.0 and 4.0, respectively. The temperature was 1.0 kBT according to

153   Groot's work.[21] Flory-Huggins parameters (χ_{ij}) were obtained in Blend module. They

154   could be converted into the interaction parameters (a_{ij}) by the equation, $a_{ij} = \chi_{ij} \times 3.27$

155   + a$_{ii}$. Table 1 shows the interaction parameters a_{ij} used in this work. The diffusion

156   coefficient of a DPD particle was interpreted as the ratio of the distance that fluid

157   particles diffused through to the time they took.[20] Larger diffusion coefficient of water

158   molecules meant lower viscosity of solutions.

8

159   **Table 1** Bead-Bead interaction parameters a_{ij} used in the simulation.

Bead	a	b	c	d	e	f	h	t	w
a	80								
b	22.9	25							
c	14	29.8	70						
d	75.4	79.1	47	25					
e	29	29.5	27.1	70.9	25				
f	90	45	16	73.3	55.3	100			
h	20	23.7	29.5	49.4	27.5	27.4	25		
t	51.7	55.9	32.3	33.1	53.5	66.1	36.2	25	
w	15	27	28	64.4	31.5	9.6	30.7	56.5	25

160

161   **3. Results and discussion**

162   **3.1. Rheological properties of the mixed solutions of HA-PAM and various**

163   **surfactants**

164

165
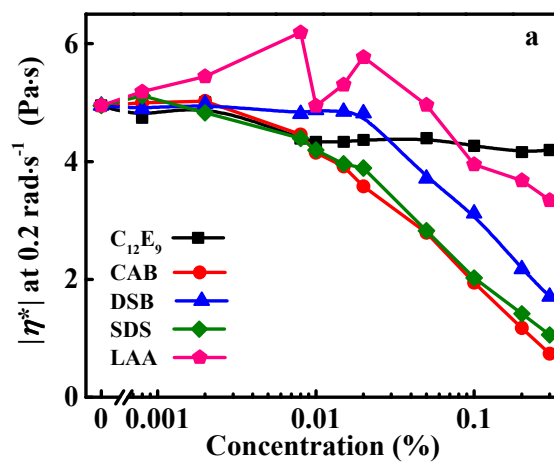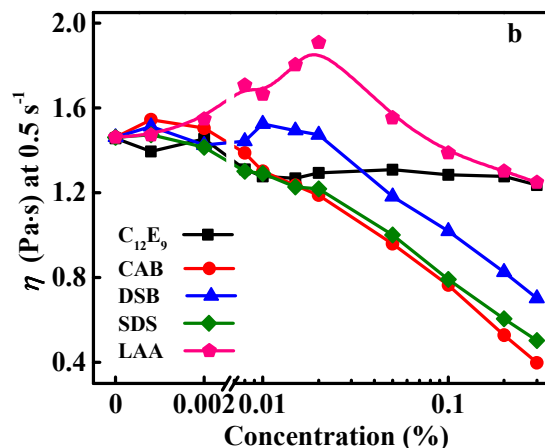
Fig. 2 Influences of various surfactants on dynamic and shear viscosity of 0.1%

HA-PAM solutions.

168

169   Fig. 2 shows the variation of the viscosity of 0.1% HA-PAM solutions with

170   concentrations of CAB, DSB, LAA, $C_{12}E_9$ and SDS. The critical micelle

171   concentrations of these surfactants are 0.045, 0.072, 0.010 (Fig. S2), 0.0058[22] and

172   0.23%,[23] respectively. $C_{12}E_9$ exhibits little effect on the viscosity of HA-PAM

173   solutions. The ionic surfactants (CAB, DSB and SDS) all induce a slight increase,

174   followed by a decrease of HA-PAM solution viscosity with increasing surfactant

175   concentrations. The slight increase of the viscosity results from the formation of

176   surfactant micelle bridges between different polymer chains. Compared with the

177   nonionic surfactant $C_{12}E_9$, the ionic surfactants induce a more abrupt viscosity

178   decrease of HA-PAM solutions at the surfactant concentration higher than 0.1%,

179   which might be because of the increase of inter- molecular electrostatic repulsion

180   induced by the co-aggregation of ionic surfactant and the screening effect of excess

181 counter ions.[24-26] Being different from the above systems, the HA-PAM/LAA （H/L）

182 combined system exhibits the strongest thickening ability at the concentration (C_a)

183 less than 0.08%. Two viscosity maximums are observed at C_a = 0.008 and 0.02%,

184 respectively.

185 **3.2. Effects of LAA concentration C_a and $\dot{\gamma}$ on the rheological properties of H/L**

186 **solutions**
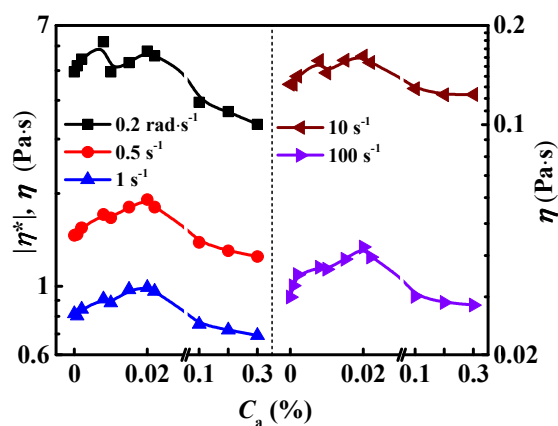
187

188 **Fig. 3** Effect of LAA concentration (C_a) on dynamic and steady viscosity of HA-PAM

189 solutions at different shear rates.

190
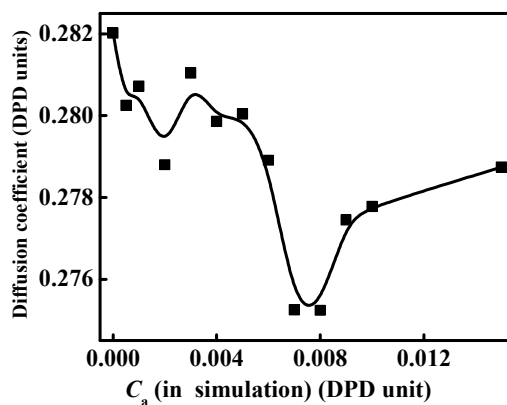
191

192   **Fig. 4** Water diffusivity in the aqueous system as a function of LAA concentration at a

193   shear rate of 0.005 in the simulation.

194

195   Fig. 3 shows the dynamic and steady viscosity of H/L solutions as a function of

196    $\dot{\gamma}$ and C_a. Similar viscosity variation trend with increasing C_a are observed at various

197    $\dot{\gamma}$ (Figs. 2 and 3), but the first viscosity maximum is less obvious under the steady

198   shear than the oscillation shear (Figs. 2 and 3). DPD simulation results of the H/L

199   solutions also show two minimums of the diffusion coefficient of water molecules in

200   the systems with increasing alkanolamide concentration in the simulation (C_a (in

201   simulation)) (Fig. 4), which agreed very well with the experiment results, indicating

202   that the bead-bead interaction parameters a_{ij} used in the simulation are reasonable.

203
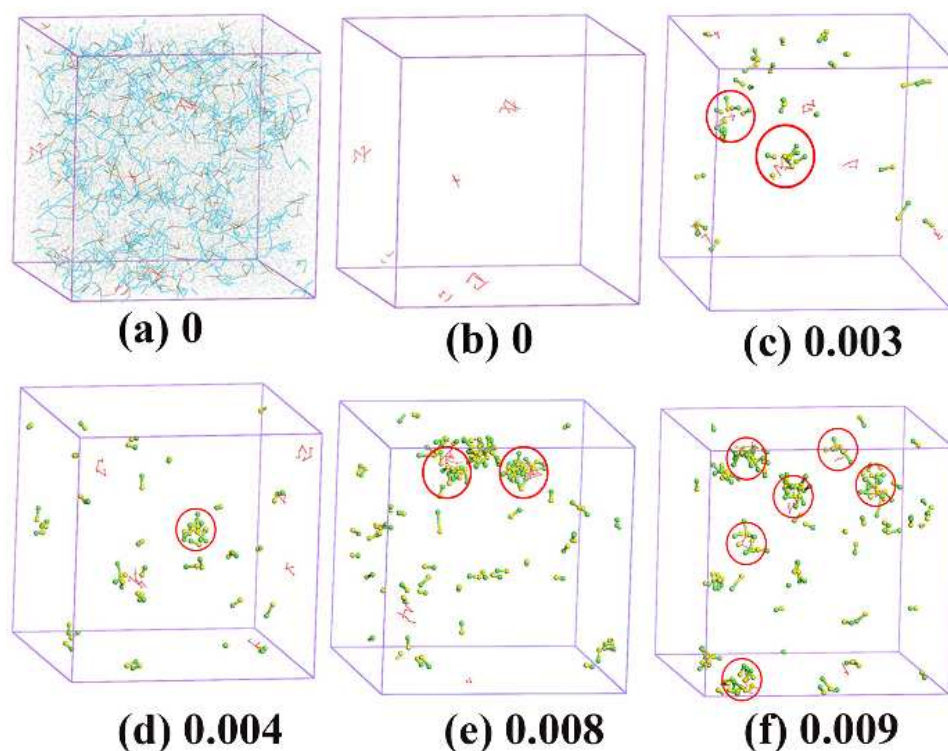
Fig. 5 Configurations of H/L at shear rate of 0.005 and various LAA concentrations: (a) 0 with all the beads; (b) 0; (c) 0.003; (d) 0.004; (e) 0.008; (f) 0.009. Colors of the beads are the same as those in Fig. 1: a (sodium acrylate, golden yellow); b (acrylamide, light blue); c and d (hydrophobically associating monomer, orange and red); and e and f (sodium 2-acrylamido-2-methylpropanesulfonate, brown and pink); h and t (surfactant head and tail, green and yellow) in the simulation;

According to simulation results shown in Fig. 5, the hydrophobic side chain of the HA-PAM molecules cluster to form microdomains (Fig. 5b). When LAA was added to the HA-PAM solutions, the LAA molecules aggregate around these hydrophobic domains (Fig. 5c), and mixed micelle-like associations containing LAA

216 molecules and hydrophobic segments of different HA-PAM molecules were formed.

217 Herein, the LAA acts as crosslinkers which contributes to the increase of the

218 intermolecular hydrophobic interaction, resulting in the viscosity increase of mixed

219 solutions (Fig. 3). Fig. S3 shows the fluorescence spectra of the H/L solutions at

220 different C_a. The increase of I_3/I_1 values with increasing C_a also means that more

221 hydrophobic microdomains were formed.

222 When the LAA concentration increases, independent LAA micelles were found

223 in the bulk phase (Fig. 5d), the desorption of LAA from the hydrophobic

224 microdomains of the polymer molecules may lead to the decrease of the viscosity of

225 the mixed solutions, as shown in Fig. 3. As the LAA concentration increases further,

226 independent micelle were formed around the hydrophobic side chains of the HA-PAM

227 (Fig. 5f).[27-29] The intermolecular association of HA-PAM molecules induced by

228 coaggregation of the hydrophobic side groups[30] would be broken, leading to the

229 viscosity decrease of the mixed solutions, corresponding well with the experimental

230 results in Fig. 3.

231
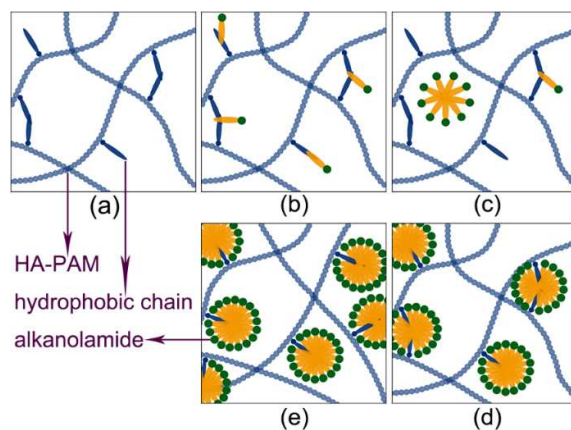
232 **Fig. 6** Schematic illustration of H/L microstructures at different LAA concentrations.

233

234   By comparing the experimental and simulation results, we conclude that the

235 LAA molecules aggregate together with the hydrophobic side chain of the HA-PAM

236 molecule, and the simulation results show that the formed aggregates containing LAA

237 micelles and hydrophobic segments of HA-PAM molecules (Fig. 5e) behave like

238 crosslinkers to bind the HA-PAM molecules together and strengthen the network

239 structure, leading to an increase of the viscosity of the bulk solutions (Fig. 3).[27-29] The

240 whole process of the effect of the LAA concentration on the micromolecular behavior

241 and the properties of the H/L mixed systems were shown in Fig. 6. At C_a < 0.008%,

242 the LAA molecules get clustered with the hydrophobic segments of HA-PAM (Fig.

243 6b). At 0.008% < C_a < 0.01%, the LAA molecules tend to form micelles in bulk

244 solution (Fig. 6c). At 0.01% < C_a < 0.02%, the micelle-like associations containing

245 LAA molecules and hydrophobic segments from different HA-PAM molecules were

246 formed (Fig. 6d), and at C_a > 0.02 %, independent micelles were formed around each

247 hydrophobic side chains of the HA-PAM (Fig. 6e).[27-29] The intermolecular association

248 of HA-PAM molecules induced by coaggregation of the hydrophobic side groups[30]

249 would be broken, leading to the decrease of the viscosity of the mixed solutions. The

250 increasing I_3/I_1 value with C_a in Fig. S3 indicates the increase of the amount of

251 hydrophobic microdomains in solutions, corresponding to the variation of the

252 microstructure shown in Fig. 5 and 6.

15

253

254
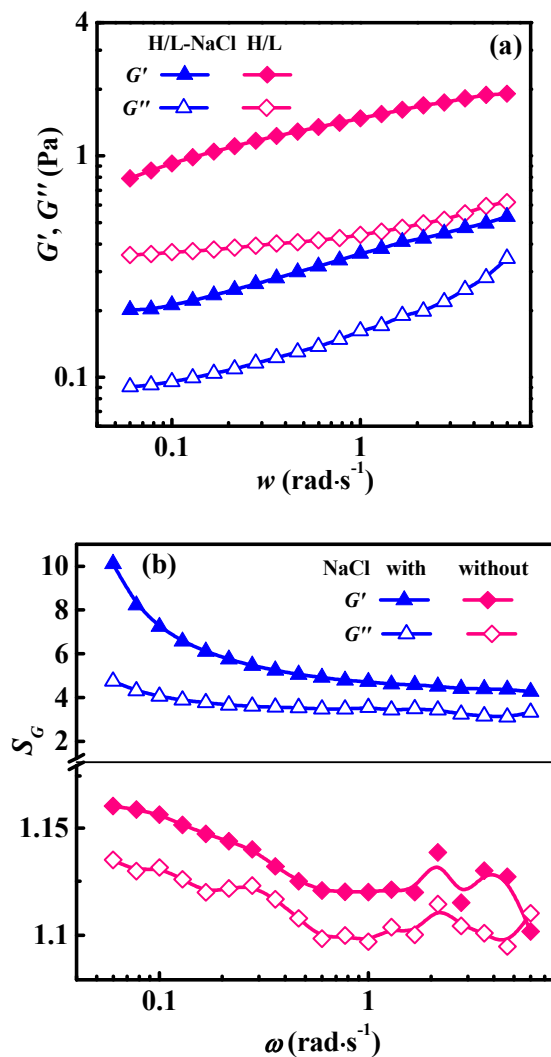
Fig. 7 (a) Frequency scan curves for H/L solutions containing 0.02% LAA and (b)

modulus ratios (S_G) of H/L to HA-PAM solutions[7] with or without 0.2% NaCl.

257

258   In the EOR area, not only the viscosity but also the elasticity of the flooding

259   solutions are important in the oil displacement process.[31] The frequency scan curves

260   of H/L solutions at $C_a = 0.02\%$ are shown in Fig. 7a. The G' are higher than G'' in the

261   studied ω range, indicating the dominant elastic behavior of the solution. Fig. 7b

262   shows the modulus ratios (S_G) of the H/L mixed solutions to HA-PAM solutions. Both

263    $S_{G'}$ and $S_{G''}$ are larger than 1, and the phase angle tangent values of the H/L mixed

264   solutions are less than those of the HA-PAM solutions (Fig. S4), indicating the

265   hydrophobic association interaction between HA-PAM and LAA also induces the

266   enhancement of the elasticity of the solutions.

267   The coaggregation of the surfactants and hydrophobic side chains of the

268   HA-PAM plays the key role in formation of the network to maintain the high

269   viscosity and elasticity of the mixed solutions. Being different from the H/L mixed

270   system, the viscosity of the mixed solutions of $C_{12}E_9$ and HA-PAM changed slightly,

271   as shown in Figure 2. The HLB of $C_{12}E_9$ was higher than LAA, and the driven force

272   for hydrophobic association is weaker for $C_{12}E_9$ comparing with LAA. It is concluded

273   that suitable hydrophilic-lipophilic balance is needed for the surfactants to get

274   coaggregated beside the hydrophobic side chains of the HA-PAM.

275   **3.3. Effect of NaCl on the rheological properties of H/L solutions**

276

277
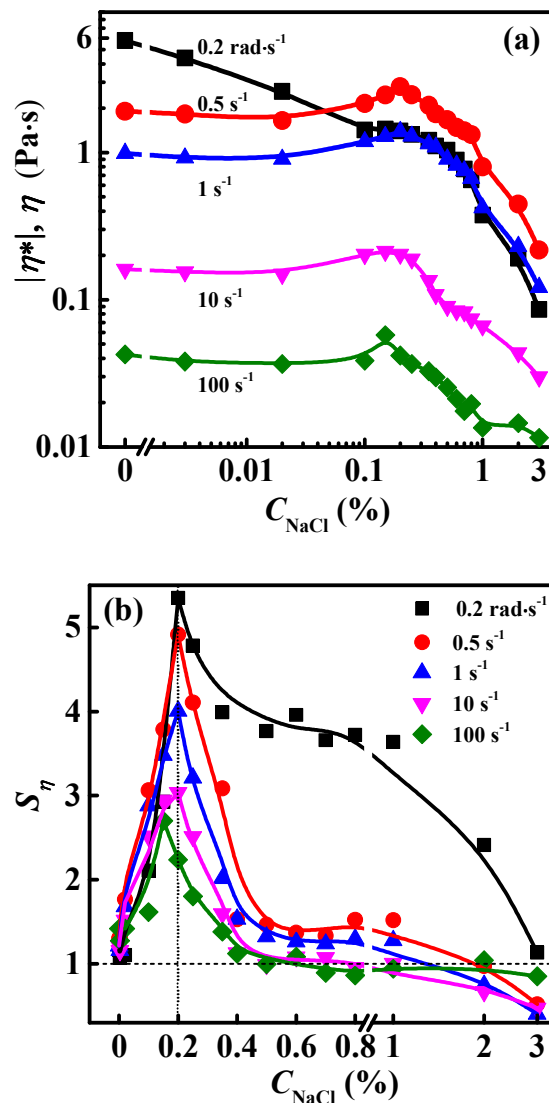
Fig. 8 (a) Dynamic (■) and steady viscosity of H/L solutions containing 0.1%

HA-PAM and 0.02% LAA and (b) interaction strength (S_η) of HA-PAM with LAA at

various NaCl concentrations and shear rates.

281

Fig. 8a shows the variation of dynamic and steady viscosity of H/L solutions

containing 0.02% LAA as a function of the NaCl concentration (C_{NaCl}). With

increasing C_{NaCl}, the viscosity of the H/L solutions exhibits the same variation trend as

18

285   the HA-PAM solutions.[7] But for the H/L solutions, a prominent viscosity

286   enhancement is observed in the presence of NaCl at $\dot{\gamma}$ = 0.5–100 s^{-1} (Fig. S5). The S_η

287   values between HA-PAM and LAA at different C_{NaCl} are shown in Fig. 8b. With

288   increasing C_{NaCl}, S_η increases first and then decreases, with a maximum observed at

289   about C_{NaCl} = 0.2% where the H/L solutions exhibit the largest viscosity (Fig. 8a). S_η

290   can decrease to be less than 1 only at very high C_{NaCl}. So the H/L binary system has

291   better salt-tolerance than HA-PAM.

292   The addition of NaCl enhanced the hydrophobic interaction between

293   hydrophobic chains of HA-PAM and LAA (Fig. 5e).[32] With increasing NaCl

294   concentration, the salting-out effect disturbs the hydration of the polymer and

295   surfactant, and thereby promotes the hydrophobic association, so S_η increases

296   continuously with the increase of C_{NaCl} at C_{NaCl} < 0.2%. Meanwhile, apart from the

297   hydrophobic units of the HA-PAM, there are several charged groups such as COO$^-$,

298   SO$_3^-$, and N$^+$ in the molecules. The screening effect of NaCl can decrease the

299   intramolecular electrostatic repulsion caused by these charged groups, leading to the

300   curling of the polymer molecules.[34, 35] The molecular curling enhances the

301   intramolecular and impairs the intermolecular hydrophobic interactions between

302   HA-PAM molecules[35], and simultaneously decreases the hydrophobic interaction

303   between HA-PAM and LAA molecules, which makes the viscosity of H/L solutions

304   decrease slightly at C_{NaCl} < 0.02 % (Fig. 8a), and S_η decrease significantly with

305   increasing C_{NaCl} at C_{NaCl} > 0.2 %. S_η < 1 at higher C_{NaCl} is probably because the LAA

306   participates in the intramolecular hydrophobic interaction of HA-PAM molecules and

307   increases the curling of HA-PAM molecules.

308   The $\dot{\gamma}$ also has a great effect on the viscosity of H/L solutions and S_η. With

309   increasing $\dot{\gamma}$, the steady viscosity of the solutions gradually decreases (Fig. 8a). At

310    $C_{NaCl} < 0.04\%$, the $|\eta^*|$ of the solutions is larger than the steady viscosity at $\dot{\gamma} =$

311   0.5–100 s^{-1}, while at $C_{NaCl} > 0.04\%$, the steady viscosity at $\dot{\gamma} = 0.5$ s^{-1} is larger than

312   the $|\eta^*|$ of the solutions, which shows that the addition of NaCl enhances the

313   shear-tolerance of the system. The shear could induce the variation of the molecular

314   conformation and coaggregation behavior. On one hand, the shear can destroy the

315   inter/intra-molecular hydrophobic interactions[36]. On the other hand, the shear can

316   inhibit the macromolecular curl. At low C_{NaCl}, the intramolecular hydrophobic

317   interaction in the H/L system is weak, so the shear principally destroy the

318   intermolecular hydrophobic interaction, which leads to the decrease of solution

319   viscosity. At high C_{NaCl}, the screening effect of NaCl induces the severe curl of

320   HA-PAM molecules, as discussed above. The shear mainly destroys the

321   intramolecular hydrophobic interaction and dissociates the LAA molecules from the

322   intramolecular hydrophobic microdomains, which makes the steady viscosities of

323   solutions at $\dot{\gamma} = 0.5$ s^{-1} higher than the $|\eta^*|$.

324   The frequency scan curves of H/L solutions with $C_a = 0.02\%$ and $C_{NaCl} = 0.2\%$

325   and S_G values are shown in Fig. 7. $G' > G''$ indicates the solution exhibits a dominant

326   elastic behavior. The $S_{G'}$ and $S_{G''}$ are larger than 1, and the phase angle tangent values

327   of the H/L solutions are less than those of the HA-PAM solutions (Fig. S4), indicating

328   the hydrophobic association between HA-PAM and LAA increases the elasticity of

329   solutions. The $S_{G'}$ and $S_{G''}$ values of solutions with NaCl are much larger than those

330   without NaCl (Fig. 7b), which reveals that in the presence of NaCl, the elasticity

331   enhancement of solutions induced by the hydrophobic interaction between HA-PAM

332   and LAA is more prominent.

333   Overall, the LAA contributes to the viscosity and elasticity enhancement of

334   HA-PAM solutions at $C_{NaCl} < 1\%$, indicating the salt tolerance of H/L solutions is

335   better than that of the HA-PAM solutions.

336   **3.4. Effect of temperature on rheological properties of H/L solutions**

337

RSC Advances

338
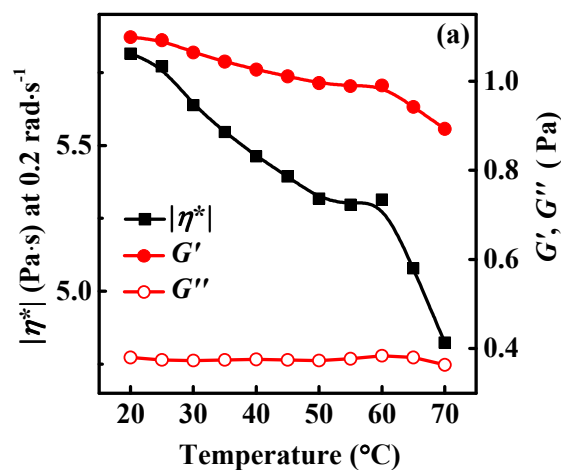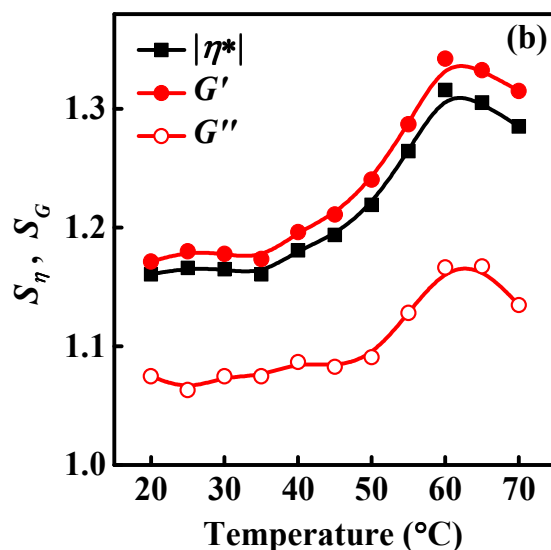
Fig. 9 Effect of temperature on (a) dynamic viscosity and moduli of H/L solutions

340 containing 0.02% LAA, and (b) viscosity and modulus ratios (S_η and S_G) of H/L to

341 HA-PAM solutions

342

343   Temperature (T) can substantially influence the rheological properties of the

344 hydrophobic associating polymer solutions.[37] Fig. 9a shows the variation of $|\eta^*|$, G'

345 and G'' with T for the H/L solutions with $C_a = 0.02\%$. G' is always higher than G'' in

346 the tested temperature range for all solutions, indicating a dominant elastic behavior.

347 With increasing T, the $|\eta^*|$ and G' of H/L solutions exhibit the similar trend as the

348 HA-PAM solutions,[7] i.e. gradual decrease, except a plateau appears at $T = 50$–60 °C,

349 respectively. The T has little effect on the G'' of solutions. The decrease of $|\eta^*|$ and G'

350 of solutions with increasing T is because high temperature accelerates the

351 macromolecular movement, thins the hydrated layer and destroys the intermolecular

352 interaction.[38] The appearance of plateaus reveals the decrease of $|\eta^*|$ and G' is

353   retarded (Fig. S6), further indicating that the hydrophobic interaction between

354   HA-PAM and LAA contributes to the viscosity enhancement of solutions.

355   In order to assess the effect of T on the interaction strength of HA-PAM with

356   LAA, S_η and S_G of solutions are shown in Fig. 9b. In the studied T range, the S_η and S_G

357   are always larger than 1, indicating the interaction between HA-PAM and LAA leads

358   to a viscosity increase. With increasing T, both S_η and S_G first increase and then

359   decrease with a maximum observed at $T = 60$ °C. As is reported, the hydrophobic

360   association is an endothermic process,[38, 39] and the increase of temperature is

361   favorable for hydrophobic interaction enhancement. Thus, The S_η and S_G increase with

362   T at $T < 60$ °C. The reduction of S_η and S_G at $T > 60$ °C is caused by the strong thermal

363   motion of the molecules which destroys the interaction between HA-PAM and LAA.

364
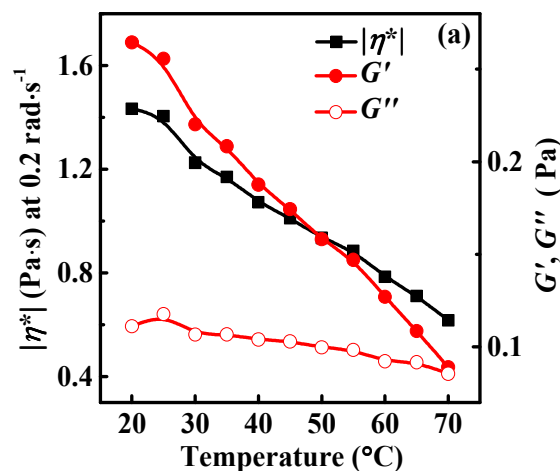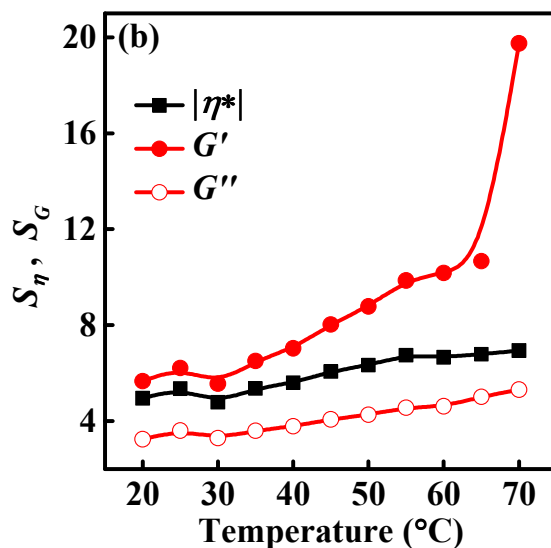
Fig. 10 Effect of temperature on (a) dynamic viscosity and moduli of H/L solutions

containing 0.02% LAA, (b) viscosity and modulus ratios of H/L to HA-PAM solutions,

with NaCl concentration of 0.2%.

In the presence of NaCl, the effects of T on the rheological properties of H/L

solutions, S_η and S_G are different from the results without NaCl. As shown in Figs. 10a

and S7, at C_{NaCl} = 0.2%, the $|\eta^*|$, G' and G'' decrease more prominently with

increasing T than those without NaCl (Figs. 9a and S6), and no plateau is observed,

which is similar with those for the pure HA-PAM solutions.[7] But G' is always larger

than G'' in the tested temperature range for the H/L solutions, indicating a dominant

elastic behavior. While for the HA-PAM solutions, G' is larger than G'' at T =

20–35 °C and less than G'' at T = 35–70 °C. Fig. 10b shows the changes of S_η and S_G

with T. All S_η, $S_{G'}$ and $S_{G''}$ gradually increase with the T in the studied range, which is

different from the results without NaCl (Fig. 9b). Besides, as the T increases from 20

24

380   to 60 °C, the S_η, $S_{G'}$ and $S_{G''}$ of solutions with NaCl increases by ~35, ~80 and ~42%,

381   respectively, while those without NaCl increases by ~13, ~15 and ~9%, respectively,

382   indicating that the hydrophobic interaction between HA-PAM and LAA was

383   enhanced in the presence of NaCl.

384   **4. Conclusions**

385   The rheological behavior of binary mixed solution of a hydrophobically

386   associating polyacrylamide (HA-PAM) and surfactants was investigated. Compared

387   with anionic surfactant SDS, zwitterionic surfactant carbobetaine ($C_{19}H_{38}N_2O_3$)

388   sulfobetaine ($C_{17}H_{37}NSO_3$) and nonionic surfactant nonaethylene glycol monododecyl

389   ether ($C_{30}H_{62}O_{10}$), the nonionic surfactant laurel alkanolamide (LAA) exhibited

390   stronger thickening ability when added to the HA-PAM solutions. The DPD

391   simulation was used to interpret the synergistic mechanism. The obvious increase of

392   solution viscosity was induced by the hydrophobic interaction between HA-PAM and

393   LAA. The effects of electrolyte concentration and temperature on the interaction

394   between HA-PAM and LAA were also investigated. The interaction strength of

395   HA-PAM with LAA enhanced with the increase of C_a, C_{NaCl} and temperature. Overall,

396   the HA-PAM/LAA mixed solution exhibited stronger salt and temperature resistance

397   than the HA-PAM solution. The HA-PAM/LAA systems are appropriate for use in

398   EOR of oil field with high salinity.

399   **Acknowledgement**

403   **References**

404   1.   H. Zhang, M. Dong and S. Zhao, *Energ. Fuel.*, 2010, **24**(3), 1829-1836.

405   2.   D. A. Z. Wever, F. Picchioni and A. A. Broekhuis, *Prog. Polym. Sci.*, 2011,

406   **36**(11), 1558-1628.

407   3.   E. E. Kathmann, L. A. White and C. L. McCormick, *Polymer*, 1997, **38**(4),

408   871-878.

409   4.   A. Sabhapondit, A. Borthakur and I. Haque, *Energ. Fuel.*, 2003, **17**(3),

410   683-688.

411   5.   C. Zhong, L. Jiang and X. Peng, *J. Polym. Sci. Polym. Chem.*, 2010, **48**(5),

412   1241–1250

413   6.   C. L. McCormick, J. C. Middleton and D. F. Cummins, *Macromolecules*,

414   1992, **25**(4), 1201-1206.

415   7.   Q. Deng, H. Li, Y. Li, X. Cao, Y. Yang and X. Song, *Aust. J. Chem.*, 2014,

416   **67**(10), 1396-1402.

417   8.   P. A. Ioannis S. Chronakis, *Macromolecules*, 2001, **34**(14), 5005-5018.

418   9.   L. Y. C. Perry F. C. Lim, S. B. Chen, *J. Phys. Chem. B* 2003, **107**(206),

419   6491-6496.

420   10.   M. Y. Thomas A. P. Seery, Thieo E. Hogen-Esch, Eric J. Amis',

421   *Macromolecules*, 1992, **25**(18), 4784-4791.

422   11.   X. Xin, G. Xu, D. Wu, Y. Li and X. Cao, *Colloid Surf. A*, 2007, **305**(1–3),

423   138-144.

424   12.   I. Hoffmann, P. Heunemann, S. Prevost, R. Schweins, N. J. Wagner and M.

425   Gradzielski, *Langmuir*, 2011, **27**(8), 4386-4396.

426   13.   K. Fukada, E. Suzuki and T. Seimiya, *Langmuir*, 1999, **15**(12), 4217-4221.

427   14.   P. Deo, N. Deo, P. Somasundaran, A. Moscatelli, S. Jockusch, N. J. Turro, K.

428   Ananthapadmanabhan   and   M.   F.   Ottaviani,   *Langmuir*,   2007,   **23**(11),

429   5906-5913.

430   15.   A. Hersloef, L. O. Sundeloef and K. Edsman, *J. Phys. Chem.*, 1992, **96**(5),

431   2345-2348.

432   16.   N. Plucktaveesak, A. J. Konop and R. H. Colby, *J. Phys. Chem. B*, 2003,

433   **107**(32), 8166-8171.

434   17.   D. Zhuang, T. E. Hogen‑Esch and Y. Zhang, *J. Appl. Polym. Sci.*, 2004,

435   **92**(2), 1279-1285.

436   18.   S. Zhang, P. Zhu, Y. Sun, Y. Yang, X. Cao, X. Song and Y. Li, *RSC Adv.*,

437   2014, **4**(79), 41831-41837.

438   19.   I. Iliopoulos, J. L. Halary and R. Audebert, *J. Polym. Sci. Polym. Chem.*, 1988,

439   **26**(1), 275-284.

440   20.   X. Cao, G. Xu, Y. Li and Z. Zhang, *J. Phys. Chem. A*, 2005, **109**(45),

441   10418-10423.

442   21.   Y. Zhao, L.-Y. You, Z.-Y. Lu and C.-C. Sun, *Polymer*, 2009, **50**(22),

443   5333-5340.

444   22.   K. S. Sharma, P. A. Hassan and A. K. Rakshit, *Colloid Surf. A*, 2007, **308**(1–

445   3), 100-110.

446   23.   S. Ghosh, S. Mondal, S. Das and R. Biswas, *Fluid. Phase. Equilibr*, 2012,

447   **332**(0), 1-6.

448   24.   K. Y. Mya, A. Sirivat and A. M. Jamieson, *J. Phys. Chem. B*, 2003, **107**(23),

449   5460-5466.

450   25.   W. Seng, K. Tam and R. Jenkins, *Colloid Surf. A*, 1999, **154**(3), 365-382.

451   26.   M. Amiri and A. A. Dadkhah, *Colloid Surf. A*, 2006, **278**(1), 252-255.

452   27.   K. Tam, W. Seng, R. Jenkins and D. Bassett, *J. Polym. Sci. Poly. Phys.*, 2000,

453   **38**(15), 2019-2032.

454   28.   G. Zhao, C. C. Khin, S. B. Chen and B.-H. Chen, *J. Phys. Chem. B*, 2005,

455   **109**(29), 14198-14204.

456   29.   X. Xie and T. E. Hogen-Esch, *Macromolecules*, 1996, **29**(5), 1734-1745.

457   30.   H. Bu, A.-L. Kjøniksen, K. D. Knudsen and B. Nyström, *Colloid Surf. A*,

458   2007, **293**(1), 105-113.

459   31.   W. Wang, Y. Liu and Y. Gu, *Colloid Polym. Sci.*, 2003, **281**(11), 1046-1054.

460   32.   J. Ma, B. Liang, P. Cui, H. Dai and R. Huang, *Polymer*, 2003, **44**(4),

461   1281-1286.

462   33.   R. Sadeghi and F. Jahani, *J. Phys. Chem. B*, 2012, **116**(17), 5234-5241.

463   34.   C. Zhong and P. Luo, *J. Polym. Sci. Poly. Phys.*, 2007, **45**(7), 826-839.

464   35.   R. D. Wesley, C. A. Dreiss, T. Cosgrove, S. P. Armes, L. Thompson, F. L.

465   Baines and N. C. Billingham, *Langmuir*, 2005, **21**(11), 4856-4861.

466   36.   K. Tam, W. Ng and R. Jenkins, *Polymer*, 2005, **46**(12), 4052-4059.

467   37.   V. D. Alves, F. Freitas, N. Costa, M. Carvalheira, R. Oliveira, M. P.

468   Gonçalves and M. A. M. Reis, *Carbohydr. Polym.*, 2010, **79**(4), 981-988.

469   38.   J. Ma, P. Cui, L. Zhao and R. Huang, *Eur. Polym. J.*, 2002, **38**(8), 1627-1633.

470   39.   J. Desbrieres, *Polymer*, 2004, **45**(10), 3285-3295.

471